FINAL TECHNICAL REPORT: 1988

Name of Grantee:	University of Washington
Principal Investigator:	R. S. Crosson K. C. Creager Geophysics Program AK-50 University of Washington Seattle, WA 98195
Government Technical Officer:	Dr. Elaine R. Padovani U. S. Geological Survey 905 National Center Reston, VA 22092
Short Title:	Earthquake Hazard Research in the Pacific Northwest
Effective Date of Grant:	February 1, 1988
Grant Expiration Date:	January 31, 1989
Amount of Grant:	$60,000.
Date Report Submitted:	June 15, 1989

Sponsored by the
U.S. Geological Survey
Grant No. 14-08-0001-G1390

CONTENTS

FIGURES

APPENDICES

Summary

This is the final technical report for USGS grant 14-08-0001-1390, "Earthquake Hazard Investigations in the Pacific Northwest". This research project has focused on a number of fundamental problems related to earthquake hazards in the densely populated Puget Sound - Willamette Valley region. We are attempting to better understand the origin of both crustal and subcrustal earthquakes in this region that is influenced strongly by the Cascadia subduction zone (CSZ), and its associated volcanic arc. To achieve this goal, we have focused on structure determination, seismicity analysis, and a study of plate kinematics. The work requires cooperation and collaboration between a number of individuals and projects, and our primary source of data is the Washington Regional Seismograph Network (WRSN).

This report is organized into four sections: tomographic imaging, seismicity and structure, kinematics and plate deformation, and earthquake hazards. Under tomographic imaging we have completed our preliminary work on the Puget Sound region, developed a new method of regularization for imaging problems, and begun attempts to jointly invert both seismic and gravity data. Under seismicity and structure, we have initiated the fitting of hypocenter data to quantitatively model the plate geometry, progressed in a study of later phases from regional and local earthquakes, and re-evaluated *b*-values for Puget Sound earthquakes. Under kinematics and plate deformation we have developed the theoretical framework necessary to quantitatively model particle flow in subduction, and done a preliminary analysis of moment release rate with respect to plate deformation. Under earthquake hazards we have begun work on a comparison of the subduction zone in SW Japan (Nankai) with Cascadia, and we have completed an article on regional seismicity (DNAG).

Appendix 1 is a preprint of an article on tomographic imaging of western Washington. Appendix 2 contains copies of recent abstracts, and Appendix 3 is a preprint of a review article on seismicity of Washington and Oregon.

Tomographic imaging

Tomographic imaging of Puget Sound region

We believe that understanding the three dimensional structure of the lithosphere is an important, fundamental part of understanding the earthquake generation process. We have carried out 3-D tomographic imaging using earthquakes as sources in western Washington as part of our efforts to obtain a clearer understanding of the structure of the continental lithosphere in this region. Previous results were published for the Mt. St. Helens region (Lees and Crosson, 1989). Recently, we have completed the initial investigation of the Puget Sound region of western Washington. This work was carried out as a dissertation project by Jonathan Lees in collaboration with Principal Investigator R.S. Crosson. A manuscript describing our results has been revised and submitted for publication in J.G.R.; it is also included as Appendix 1 of this report. We believe that these results provide insight into the distribution of accreted terranes in the overlying continental block of western Washington. There is evidence that the Eocene Crescent terrane extends at depth westward beneath southern Puget Sound, and that the irregular concentration of these rocks in the southern Puget basin coincides with a region of low crustal seismicity. Our recent attempts to add gravity constraints to the velocity inversion show promise of providing even better reconstruction of the lateral structure of the shallow crust (see details this section).

Regularization

Most tomographic image reconstructions in seismology are based on least squares or modified least squares techniques. So called "row action" methods such as back projection or Gauss-Seidel iteration may only approximate a least squares solution without requiring all of the computational machinery and effort of a full least squares approach. In tomography, the earth is usually divided into fairly small blocks for purposes of formulating and linearizing the inversion computations. Since there are certain components of the model that are invariably poorly constrained, or perhaps not constrained at all, it is necessary to apply some kind of mathematical constraint to keep the least squares computations stable. For example, a block in the model that is not sampled by a ray can assume any velocity value without affecting the observations. Normally

such blocks are constrained to have zero perturbation from the assumed background velocity. Particularly troublesome are blocks that are poorly sampled in the model, since these can give rise to large model variations (in unconstrained computations) due to noisy observations. Standard methods of constraining or "regularizing" the model include the use of smoothing operators directly on the model between iterations, and the use of "damped least squares" or Levenburg-Marquardt least squares. More recently, the use of the two-dimensional Laplacian as a roughening operator has also been tried. These techniques do not always yield satisfying results, and it is difficult to specify precisely what is being done to the model.

Recognizing the general tradeoff demonstrated by Backus and Gilbert between model smoothness and variance of the estimates, no general theory has emerged to guide the choice of smoothing in a physically satisfactory manner. A natural and physically justifiable way to enforce model smoothness is to specify the allowed part of the model wavenumber domain; i.e., the lower portion of the wavenumber spectrum of the model. Such an approach can be implemented by considering the model to be set of digital "samples" of the real earth, and designing a digital filter that will "pass" the desired part of the wavenumber spectrum. In our work, we show how to proceed from such a wavenumber filter specification, to the least squares constraint equations (Crosson and Lees, 1989). The method is straightforward, and leads to a precisely formulated and physically justifiable answer with excellent numerical stability. The filter operator is designed in the wavenumber domain using standard digital filtering techniques. The least squares computations can be implemented in a very efficient manner with standard conjugate gradient algorithms.

Our method provides a clear explanation of why the Laplacian operator is a fairly effective regularization operator, and also provides an interpretation of the action and limitations of Levenburg-Marquardt inversion. Under certain conditions on the invertability of the filter operator, the method can be shown to be formally equivalent to a method termed "convolutional quelling" by Meyerholtz, et al. (1989). However, we believe that our method is intrinsically more stable, easier to physically justify, computationally more efficient, and does not require conditions on the invertability of the filter operator. In particular, filter operators of most interest, i.e, those

that suppress a particular portion of the wavenumber spectrum, will be inherently nearly singular, making the two methods different in practice. Although the method is applicable to all types of inversion and model fitting problems, for example fitting of 2-D curves to data points, a practical requirement of the method is that the model must be parameterized with equally spaced samples. This poses no limitation in tomographic problems, since uniform sized blocks or pixels are normally used, and many types of inversion problems can also be formulated in this manner. We have tested the method in 2-D and 3-D curve fitting, and in 2-D tomographics problems, with excellent results. The method was presented at the Fall '88 AGU meeting, and we are in the process of preparing a manuscript for journal publication.

Joint Tomographic Inversion Using Gravity and Seismic Data

We have recently been working on techniques to incorporate auxiliary geophysical data sets into our seismic inversions. A regional Bouguer gravity anomaly for instance, is often expected to reflect structures obtained from velocity inversions alone. It is desirable, if possible, to interject this information into the inversion process simultaneously with the seismic data if the gravitational constraints can be satisfied without significantly degrading the fit to the seismic data. If this can be accomplished, and the resulting model differs noticeably from the model obtained from seismic data alone, it implies that the maximum in the probability space of seismic models may be a broad feature, and satisfying the gravitational constraints simply moves the solution to another position on that broad maximum. Alternatively, but less likely, including the gravity data could move the solution to an entirely different maximum of nearly equal magnitude in probability space.

In order to invert seismic and gravity data simultaneously for a single set of parameters we must assume some relationship between velocity and density. A simple and effective relationship is a direct linear relationship with coefficients constant throughout the medium (i.e. Birch's Law)

$$V_p = a + b\rho \;\rightarrow\; \Delta V = blip. \tag{1}$$

Since we deal with slowness, s, instead of velocity, V, we use the relationship

$$V = \frac{1}{s} \;\rightarrow\; \Delta V = \frac{-1}{s_o^{\,2}}\Delta s \tag{2}$$

where s_o represents the background slowness. $d\rho$ is related to the vertical component of the Bouguer gravity anomaly, dg_z, for an infinitesimal mass dm through the equation

$$dg_z = \frac{Gzdm}{r^3} \tag{3}$$

where z and r are defined in Fig. 1, and G is the gravitational constant. To obtain the perturbation due to an entire model of constant density blocks equation (3) integrates to become

$$\Delta g_z = \int_{model} \frac{Gzdm}{r^3} dxdydz - \sum_i G\,\Delta\rho_i \int_{block_i} \left[\frac{z\,dxdydz}{(x^2+y^2+z^2)^{3/2}} \right]. \tag{4}$$

Substituting for $\Delta\rho_i$ in equation (4) from equations (1) and (2) and rearranging gives

$$\Delta g_z = \sum_i \left[\frac{-G}{bs_o^{\,2}} \int_{block_i} \left[\frac{z\,dxdydz}{(x^2+y^2+z^2)^{3/2}} \right] \right] \Delta s_i \tag{5}$$

where, since our gravity data is sampled at regular intervals equal to the horizontal block size, the integral over each block need be calculated only once and kept in a look-up table. Everything in the square brackets can be lumped into one term which will simply be the coefficients of a sparse matrix, Ω, representing the partial derivative of vertical gravitational acceleration perturbation with respect to slowness perturbation. The matrix is sparse since we do not need to integrate over the entire model, but only over blocks in the region relatively near the point of measurement. This is illustrated two-dimensionally in Fig. 1. where each successively dark shade represents the minimum density perturbation required for a given block to produce a vertical gravity anomaly of at least 1 mgal at the measuring point. This explains why shallow layers often dominate the short and middle wavelength features of gravitational inversions, particularly when damping has been introduced. This is even more pronounced in joint inversions since the seismic data tends to have lower resolution in these shallow regions, and therefore is more amenable to changes there.

Combining equation (5) with the usual seismic constraint equations, $\mathbf{A}\Delta\mathbf{s} = \Delta\mathbf{t}$, and smoothness constraints, $\mathbf{F}\Delta\mathbf{s} = 0$, results in the system of equations

$$\begin{bmatrix} \mathbf{A} \\ \lambda\mathbf{F} \\ \gamma\Omega \end{bmatrix} \Delta\mathbf{s} = \begin{bmatrix} \Delta\mathbf{t} \\ 0 \\ \Delta\mathbf{g} \end{bmatrix} \tag{6}$$

where λ and γ are trade-off parameters weighting the relative importance of the various

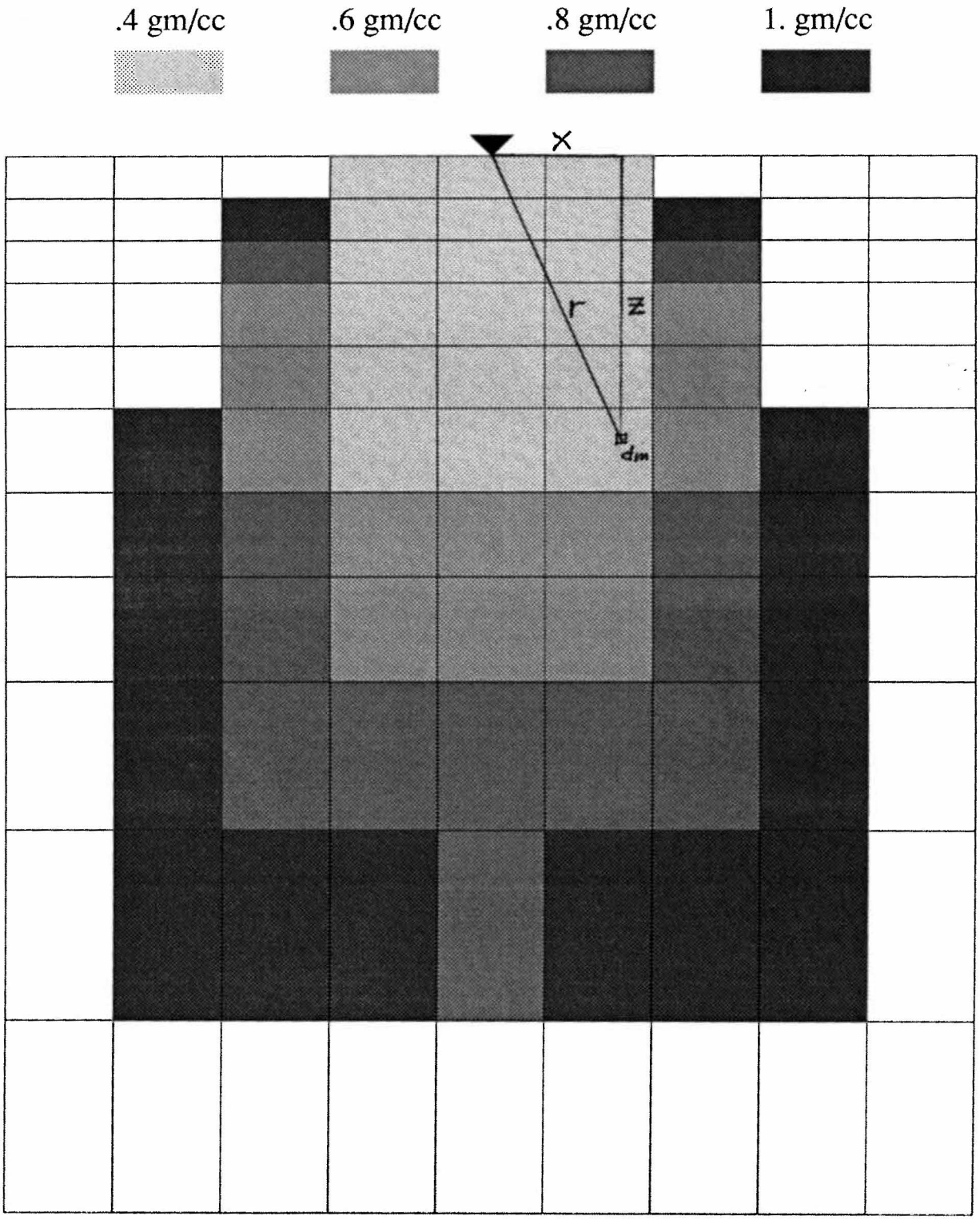

Figure 1. Schematic cross section of density block model. Each successively dark shade represents the minimum density perturbation required for a given block to produce a vertical gravity anomaly of at least 1 mgal at the measuring point.

constraints. With the examples which we have used to date, we have found that the gravitational constraints can be nearly completely satisfied (variance reductions of over 95%) without severely effecting the variance reduction of the seismic constraints (typical changes are from 34% variance reduction to 32%). Since gravity data typically contain smoother variations than seismic, there will be a trade-off between the gravitational and smoothing constraints. We are therefore investigating the two-dimensional surface of the trade-off between these parameters using cross-validation techniques.

Results of our preliminary analysis of the use of this technique in the Puget Sound region have been very encouraging (Lees and VanDecar, 1989). As mentioned previously, the regional gravity data, which includes some of the largest gradients known, can be almost completely satisfied without seriously degrading the degree to which the seismic constraints are satisfied. This demonstrates that in some regions, even with the assumption that Birch's Law holds strictly, models can be generated which satisfy both data sets. In other regions, where Birch's law does not hold, this technique cannot be applied. For example, in Eastern Washington, shallow layers of Columbia Plateau basalts seem to have lower densities but higher seismic velocities than some of the sedimentary structures in the region (Rodi et al., 1980). This is a case where, at least for the very shallow layers, Birch's law may actually be reversed. Thus the technique of joint inversion must be applied cautiously, and the velocity and density parameters possibly decoupled in shallow model layers.

Seismicity and Structure Investigations

Structure Refinement from Hypocenter Data

Seismicity and structure studies are closely related since seismicity information is used to infer certain structure characteristics of a region. In subduction zones, seismicity is most often the definitive data used to trace the broad features of subducted slabs. The Cascadia subduction zone is generally seismically quiescent, except in the vicinity of Puget Sound, where a clearly defined Wadati-Benioff zone is observed. The arch structure proposed for the Juan de Fuca slab (Crosson and Owens, 1987; Weaver and Baker, 1988) in the vicinity of Puget Sound was based in part on

careful analysis of hypocenter locations within the (inferred) subducted slab.

For many purposes, we need a quantitatively defined representation of the slab geometry. Such a model could consist of a grid of depths to a slab interface (e.g. Moho) over a specified region. This model is needed for quantitative analysis of slab kinematics and for future analytical modeling of the subduction zone processes. In an attempt to quantitatively define the slab structure, we are currently carrying out analytical surface fitting to the slab hypocenter distribution. This work requires careful relocation and selection of the highest quality hypocenter observations. Since the slab hypocenters appear to occur throughout a finite slab thickness, we have developed an algorithm to automatically select events near the top of the distribution in order to mathematically model the "boundary" at the top of the seismogenic zone. We have developed a non-parametric surface fitting procedure, and can incorporate independent data such as that derived from our teleseismic P waveform studies into the surface fitting. This work is continuing, and, although promising, has not yet produced an improved quantitative description of the slab geometry.

Later Phases from Local Earthquakes

An unexploited but potentially rich source of additional information on the structure of the subduction zone is the analysis of later phases in seismograms from local earthquakes. Ivar Mundal and Mooto Ukawa (visiting scientist from Japan), are collaborating in an initial phase of this research. From extensive studies of the subducted Philippine Sea plate beneath southwest Japan, Ukawa and his colleagues have been able to identify S phases that are trapped within the subducted oceanic crust, a dipping low velocity channel within the subduction complex. This work is based on careful identification of apparent velocity, wave polarization, and energy modeling (Hori, et al., 1985). In order to get significant trapping of energy within the oceanic crustal layer, the hypocenters of earthquakes must also lie within the same layer. This study provides perhaps the most certain identification of the oceanic crustal layer as a source of earthquakes in southwestern Japan. We have looked carefully for the analog of the Japanese observations from seismograms from local and regional earthquakes from the WRSN. Our efforts have been hampered somewhat

by not having 3-component seismograms from which clear identification of S phases is possible. Although we are certain the structure of the subduction zone contains the same low velocity oceanic crust as in southwest Japan, to date we have only observed a small number of events that might be candidates for the production of trapped phases, and our preliminary conclusions are that most, if not all of the intraslab earthquakes occur beneath the oceanic crustal layer. This preliminary result agrees with the tentative conclusion of Crosson and Owens (1987) that the intraslab earthquakes lie beneath the subducted oceanic Moho. We have discovered other unusual phases associated with intraslab earthquakes that we have not yet adequately interpreted. Further analysis of these data should be very important in gaining an increased understanding of the subduction zone structure.

b-Values for Puget Sound Region Earthquakes

In an additional seismicity study we have reexamined the recurrence information for Puget Sound earthquakes using a 17 year interval of high quality network data from 1972 to 1988. This investigation has produced some interesting results. Earthquakes in the Puget Sound region occur in two distinct, spatially separated zones with unequal recurrence statistics. The deep zone is interpreted to lie within the subducted Juan de Fuca slab (intraslab), and the shallow zone is interpreted to be totally within the overlying continental lithosphere (intracontinental). The period from 1972 to 1988 includes the highest quality coda-determined magnitudes for western Washington. We separated the events into slab and continental earthquakes using a dividing plane that passes along the seismically quiescent zone between the subcrustal and crustal earthquakes. Distinctly different *b*-values are obtained for the two zones: 0.57 for the deep (slab) and 1.00 for the shallow (crustal) earthquakes. These relationships are shown in Fig. 2. The largest Puget Sound region earthquakes, such as the 1949 Olympia event, have all apparently occurred within the intraslab zone. If we extrapolate the curve to 10 times the 17 year period of observation (170 years) the result is magnitude 7.4, a value often considered to be near the maximum observed for intraslab earthquakes. However, this curve shows a marked saturation above about magnitude 3.7 which places considerable uncertainty on the validity of any extrapolation. Saturation is often

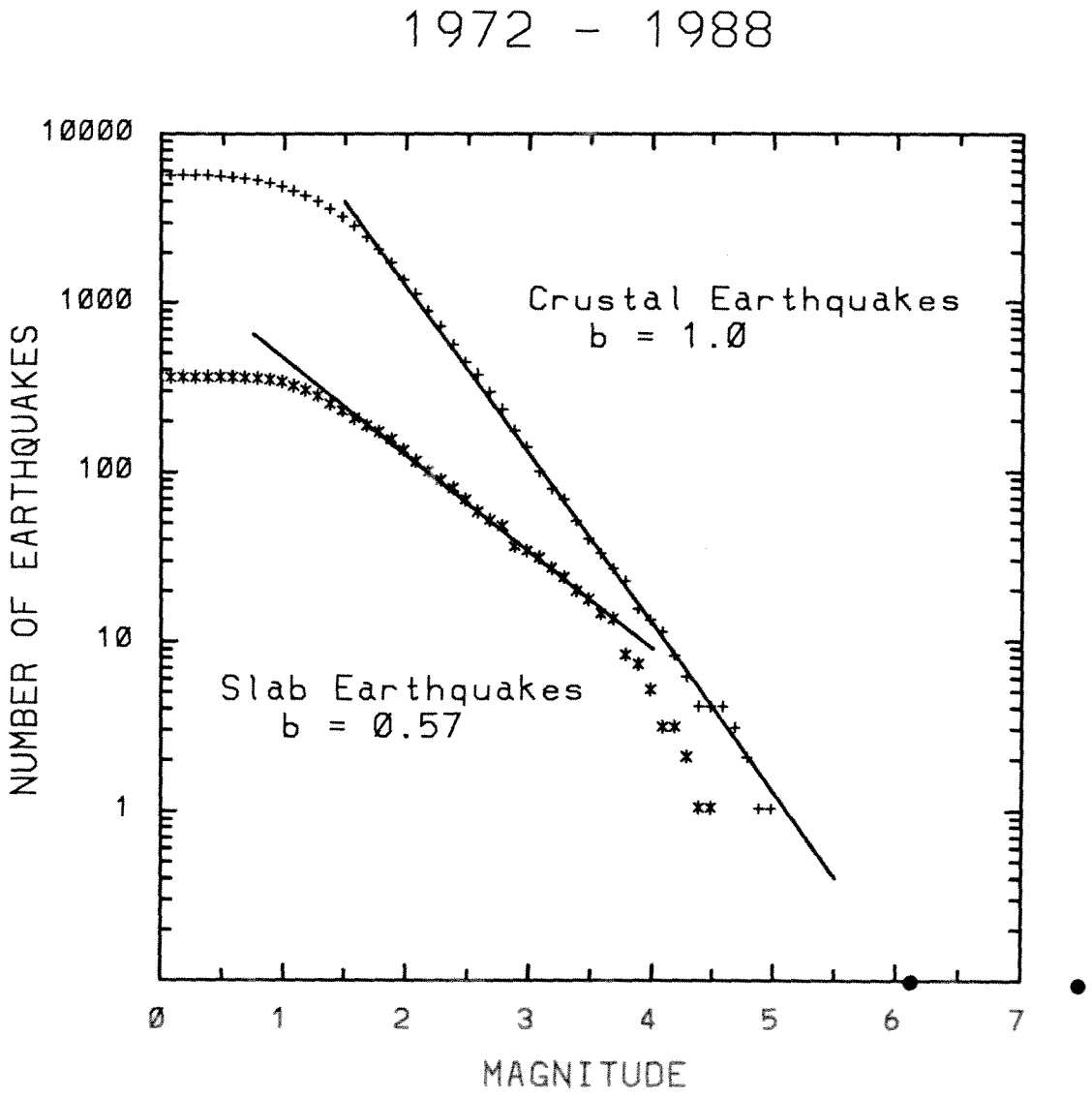

Figure 2. *b*-values the two seismogenic zones in western Washington determined using coda magnitudes of earthquakes from 1972 to 1988. Slab and continental earthquakes were separated using a dividing plane that passes along the seismically quiescent zone between the subcrustal and crustal earthquakes. *b*-values are distinctly different for the two zones: 0.57 for the deep (slab) and 1.00 for the shallow (crustal) earthquakes.

explained as the effect of some natural physical length scale limitation, and the plate thickness might play such a role in this case. If so, explanation of events as large as the 1949 M 7+ Olympia earthquake becomes extremely difficult. We speculate that the intraslab microearthquakes that occur regularly beneath Puget Sound basin may reflect processes at a fundamentally different scale than those of large earthquakes such as the 1949 Olympia event. Understanding this difference is a significant challenge that lies ahead.

For the crustal earthquakes, we have excluded the Mt. St. Helens, Elk Lake, and Goat Rocks sequences since they can be interpreted as classic aftershock sequences which would dramatically distort the recurrence curve. Crustal earthquakes do not exhibit the saturation effect. Again, extrapolating the crustal sequence of earthquakes, a 170 year mean recurrence interval for a magnitude 6.1 earthquake is found. These estimates are derived for restricted regions of high seismicity within the Puget Sound basin, roughly a 40,000 km^2 region.

Coordination with other Structure Studies

Using well located earthquake hypocenters and P waveforms from teleseisms recorded on a portable broadband profile south of Puget Sound, we hypothesized a broad arch structure for the subducted Juan de Fuca plate beneath the Puget Sound area (Crosson and Owens, 1987). The method that we used to analyze the data has come to be known as the "receiver function" approach, since the 3-component data are deconvolved to produce seismograms that are characteristic primarily of the structure at the receiver location. The slab geometry that we proposed is approximately consistent with deformation required to conserve surface area of the slab while accommodating the trench bend near 47° N latitude. Most of the earthquake hypocenters that occur within the subducted Juan de Fuca slab lie in the central Puget Sound basin, away from the localities of our original receiver function sites, so direct association of the receiver function structure with earthquake hypocenters was not possible in our original efforts. Thus we could not identify with certainty the seismogenic portion of the subducted slab, although reasonable results are obtained when we assume that it is mainly the brittle upper mantle of the slab. To establish this association, and to directly test our slab model, we are carrying out the receiver function

analysis, under NSF project support, at several stations established in a NS profile in the central Puget Sound basin. The success of this work depends critically on coordination with the hypocenter relocation and interpretation efforts of this project. Due to the large number of intraslab earthquakes in this region, the experiment should allow us to test our slab geometry model and to directly identify the seismogenic part of the slab.

Kinematics and Plate Deformation

A primary goal of this study is to obtain a better understanding of seismic observations in terms of deformation or three-dimensional flows. Clearly, knowledge of slab shapes is not sufficient information to determine strains. Our approach is to investigate plausible kinematic flows, starting with those which produce the minimum amount of kinematic deformation. In order to proceed, we need a measure of deformation. An obvious measure is the volume integral of the square of the effective strain rate (the deformation tensor dotted into itself):

$$\varepsilon^2 = \int_V \mathbf{D}:\mathbf{D}\,dV = h\int_A \mathbf{D}^0:\mathbf{D}^0\,dA + \frac{h^3}{12}\int_A \mathbf{D}^1:\mathbf{D}^1\,dA \qquad (1)$$

We have expanded the deformation (strain-rate) tensor of an assumed steady state, incompressible flow in a Taylor series expansion with respect to the direction normal to the local slab tangent:

$$\mathbf{D}(n) = \mathbf{D}^0 + n\mathbf{D}^1. \qquad (2)$$

$\mathbf{D}^0$ and $\mathbf{D}^1$ each vary as a function of position on the surface of the slab. It can be shown that $\mathbf{D}^0$ is the in-plane strain-rate tensor describing changes in area and shearing in the plane of the slab. $\mathbf{D}^1$ is a generalized bending strain-rate tensor. Integrals over V are over the volume of the slab, and over A are over the area of the slab whose thickness is h. Note the scaling factor of $h^2/12$ that weights the relative importance of the in-plane versus bending strain rates. In the limit of narrow slabs, the in-plane strain rates dominate.

Power Law Rheology

If we assume a constant viscosity Newtonian rheology within the slab then ε^2 of (1) is proportional to the global integral of the dissipation power associated with deforming the slab. On the other hand, if the slab has a power law rheology with power n then the total dissipation power is proportional to ε_n^2 where

$$\varepsilon_n^2 = \int_V (\mathbf{D}:\mathbf{D})^{(1+\frac{1}{n})/2} dV \tag{3}$$

By minimizing (3) using a variety of values of n we can simulate many different types of material behavior. For n=1 the material behaves as a Newtonian fluid and (3) reduces to (1). In the limit as n goes to infinity (3) amounts to minimizing the global average of effective strain rate (one-norm) and approximates plastic behavior or one in which friction on faults is important [e.g., Houseman and England, 1986]. n=3 is appropriate for a lithosphere dominated by the power law creep observed in olivine [Goetze, 1978]. As n varies from 1 to ∞ the minimization varies effectively from a two-norm to a one-norm of the deformation tensor components. Whereas the two-norm will attempt to prevent large strains anywhere, the one-norm is much more tolerant of large strain rates and may allow tears or isolated large strains, putting them where the geometry requires, without the investigator needing to decide where tears belong.

Boundary conditions

Calculations are carried out in a coordinate system in which the trench is fixed. We assume that a spherical shell of oceanic lithosphere enters the trench at the relative plate motion velocities. It is less clear how to specify the kinematic boundary conditions along the edges and bottom of the slab; to date we have assumed free boundary conditions.

Example of two-dimensional plate-bending

Previous studies in the geophysical literature on plate bending have considered a variety of rheologies including, elastic, viscous, viscoelastic and elastic-perfectly plastic [eg. Caldwell et al., 1976, McAdoo et al., 1978; Chapple and Forsyth, 1979], but all are restricted to infinitesimal vertical displacements from an initial horizontal plate. As the plate subducts to a finite dip, the plate-

normal vector rotates and the simple plate bending equations must be cast in curvilinear coordinates that follow the plate geometry. Kawakatsu [1986] discussed strain rates from unbending slabs and produced a simple formula for estimating their magnitudes (see also, Tsukahara [1980]). This approach is useful for order-of-magnitude calculations, but as we will show below, does not match all the geometric boundary conditions.

For two-dimensional flow, with the slab shape given, the particle velocity in the along-arc direction and slab normal directions are zero, and the only free parameter is the particle speed as a function of position in the down-dip direction. The in-plane strain-rate tensor contains only one non-zero eigenvalue which equals $\partial u/\partial s$, where s is the spatial coordinate in the local down-dip direction and u is the particle speed. Thus, the in-plane strain rates vanish if the particle speed is everywhere constant regardless of the 2-D slab shape. In this case the bending strain-rate tensor also has only one non-zero eigenvalue (with associated eigenvector in the $\hat{s}$ direction) and it reduces to $nu\partial\kappa/\partial s$ where n is distance from the slab, and $\partial\kappa/\partial s$ is the spatial rate of change of slab curvature. This deformation represents pure bending. If the curvature is constant ($\partial\kappa/\partial s$ = 0) the flow is a simple rotation with no deformation. Deformation occurs during bending from the trench to the point of maximum slab curvature and from unbending below that depth. The direction of maximum extension or compression is the down-dip direction, and for a slab that is unbending are compressive above and tensional below the mid-plane (eg. Japan double Wadati-Benioff Zone).

We have extended our calculations to two-dimensional plate bending by determining the slab shape that minimizes global strain energy (1):

$$\varepsilon^2 = \frac{u^2 h^3}{12} \int (\partial\kappa/\partial s)^2 ds \qquad (4)$$

subject to the six boundary conditions of slab position, dip, and curvature evaluated at the trench and at some depth deep in the mantle. An analytic solution is obtained using calculus of variations, but is in terms of curvature as a function of position along the path s. We are developing numerical techniques for determining the solution that matches the specified boundary conditions.

Example of three-dimensional in-plane strains

In the limit as slab thickness (h) goes to zero, in-plane strains dominate over bending strains (1). In this example, we specify slab shape and compute the kinematic flow field u on S that minimizes ε^2 (1). Consider a set of N particles distributed along the trench and subducting into the predefined slab geometry along flow paths specified initially by the relative plate velocities. For a small time step the particles are subducted down the slab using an initial guess of the particle motions.

We allow for arbitrary variations of the velocity field u within the plane of the slab, S, by perturbing, from the initial guess, the speed and subduction azimuth of each of the N particles, forming a perturbation vector $\Delta\mathbf{X}$ of length 2N. Using the initial guess for the flow field it is straight forward to calculate the deformation tensor $\mathbf{D}_i^0$ at each of the N points indexed by i. The 9N components of the N deformation tensors are stored in the vector $\mathbf{S}$. Let $\mathbf{A}$ contain the partial derivatives of the deformation tensor with respect to the components of the perturbation vector. We solve $\mathbf{A}\Delta\mathbf{X} = \mathbf{S}$ for $\Delta\mathbf{X}$ by least squares and iterate to determine the flow field that minimizes the quantity $\mathbf{S}^T\mathbf{S}$.

$$\mathbf{S}^T\mathbf{S} = \sum_{i=1}^{N} \mathbf{D}_i^0 : \mathbf{D}_i^0 \tag{5}$$

Thus, the solution is the flow that globally minimizes kinematic deformation integrated over all particles for one time step. The process is repeated sequentially for each time step. This approach closely approximates solving for the flow that globally minimizes (5), which is an integral over the area of the entire slab.

Taking advantage of the symmetries in the deformation tensor and the sparseness of the $\mathbf{A}$ matrix, we use LSQR [Paige and Saunders, 1982] to solve the inverse problem. On a SUN4 workstation these calculations seldom take more than an hour, allowing a great deal of flexibility in exploring realistic slab geometries and the effects of varying the geometry. It is straight forward to solve (3) by nonlinear least squares to investigate the effects of other rheologies such as

power law and plastic on the deformation.

Seismic moment versus strain rate

Seismic moment M_0 of a double couple earthquake is a simple kinematic quantity defined by the shear modulus m, the area of the fault plane A and the average amount of slip on the fault s:

$$M_0 = \mu A s \tag{6}$$

Brune [1968] used the linearity of this relation to estimate the mean rate of seismogenic slip v along a subduction thrust zone by summing the moment of large thrust earthquakes in a time interval T and over the area of the entire thrust zone:

$$v = \frac{\sum M_0}{\mu A T} \tag{7}$$

The mean rate of slip closely approximates the relative plate rates in many subduction zones. A similar analysis can also be used for intraplate deformation [eg. Bevis, 1988]. Consider several earthquakes occurring during time T, evenly distributed throughout a volume V of slab with identical down-dip compressive focal mechanisms. If the slip is evenly distributed between the two nodal planes, the deformation represents an in-plane strain with down-dip shortening and no along-arc strain. The down-dip component of strain rate is given by:

$$D = \frac{\sum M_0}{2\mu V T} \tag{8}$$

The expression for the mean bending strain rate is identical. This allows a comparison between the total strain rate in a portion of the subducting slab and the theoretical minimum strain rate. We find that the observed lateral variations in seismic moment are as dramatic as the vertical variations discussed at great length in the literature [eg. Vassiliou et al., 1984].

Preliminary Application to the Cascadia Subduction Zone

The spatial distribution of seismicity, interpreted to lie within the descending Cascadia slab, defines an arch-like structure [eg. Crosson and Owens, 1988] characterized by a shallow dip

(~10°) from the trench to Puget Sound, and a steeper dip (~20°) beneath Oregon to the south and Vancouver Island to the north. Coincident with the arch axis is an increased level of seismicity in the vicinity of the Olympic Peninsula and Puget Sound, both in the slab and the overriding plate. The arch is landward of a concave oceanward bend in the trench, a curvature that is backwards relative to most trench/arc systems. Like a table cloth hanging over the corner of a table, the Cascadia slab contains more material than the geometry can easily accommodate. A table cloth normally falls into a series of tight pleats at the corner, which can be straightened out by pulling the corner out at a shallow dip. Each of these geometries contain no in-plane strains (the table cloth is neither ripped nor stretched), but the smooth arching configuration reduces bending strains. Fig. 3 shows the kinematic flow that minimizes in-plane strains associated with subducting a spherical shell of oceanic lithosphere into a slab geometry characterized by a 20° dip along all cross sections normal to the trench. The strain rates are largest and compressive along strike beneath the Olympic Peninsula and Puget Sound, where the slab is seismically active. Strain rates, which reach values of $2\times10^{-16}s^{-1}$, can be reduced by a factor of two by allowing the slab to arch with a 10° dip along its axis, suggesting that both the arch and the seismicity distribution may be natural consequences of the trench geometry.

We have also calculated the minimum amount of bending strain rate (4) associated with 2-D bending and unbending the slab to leave the trench at the appropriate position and dip, pass through the slab seismicity, and reach the steep dip (65°) required to fit the teleseismic tomography results of Rasmussen and Humphries [1988] (Fig. 4). For a seismogenic slab thickness of 10 km, this slab shape requires a mean bending strain rate of $2\times10^{-16}s^{-1}$ which should be interpreted as the minimum amount of bending strain rate required of the slab. Some of this deformation could, of course, occur aseismicly.

During the last 40 years, the seismic moment release from intraslab Cascadia earthquakes has been dominated by the 1949 Puget Sound (M_0 = 1.5×10^{26} dyne-cm [Baker and Langston, 1987], m_B = 7.1 [Astiz et al., 1988]) and 1965 Seattle (m_B = 6.9 [Astiz et al., 1988]) earthquakes. Distributing the summed moment of these and other slab events over an area of 200×200

Cascadia Slab

Intraplate Seismicity

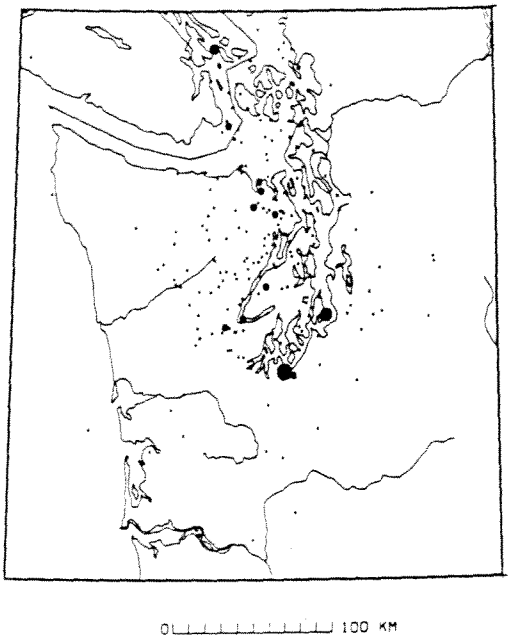

Slab Geometry

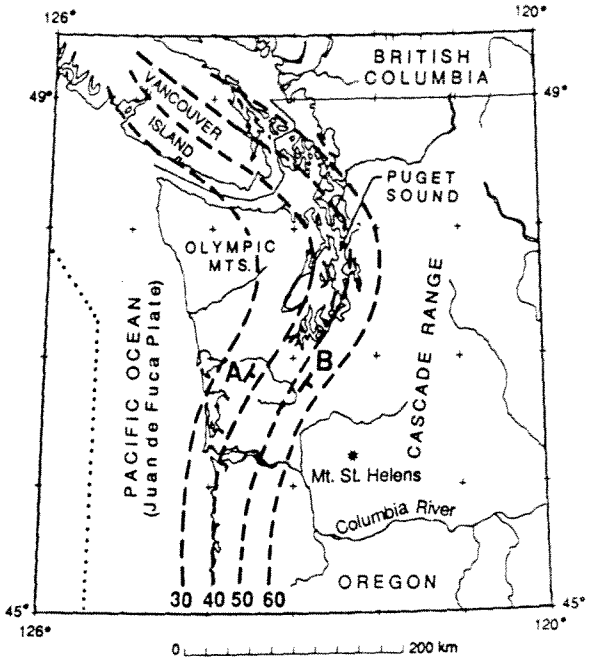

Predicted Strain Rates

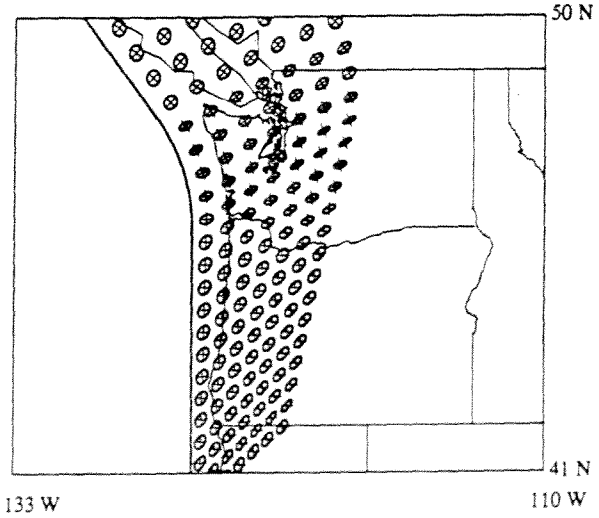

Fig 3. (top left) Map showing epicenters of events interpreted to lie within the downgoing Cascadia slab. Small dots are events with $m_b<4$. Large dot size is scaled by event magnitude. (upper right) Contours of the slab geometry estimated from seismicity, teleseismic P-to-S conversions off the subducted oceanic moho, and seismic reflection lines (from Crosson and Owens [1987]). (bottom) In-plane strain rate ellipses calculated using equation (1) and a simplified slab geometry whose dip is everywhere 20°. Short axes of ellipses represent the compression direction which is greatest in the along-arc direction near Puget Sound. The along-arc compression, which reaches strain rates of 2×10^{-16} s^{-1}, is reduced by a factor of two when the slab is arched under Puget Sound as shown in upper right. The seismicity is concentrated in the region of predicted high strain rates.

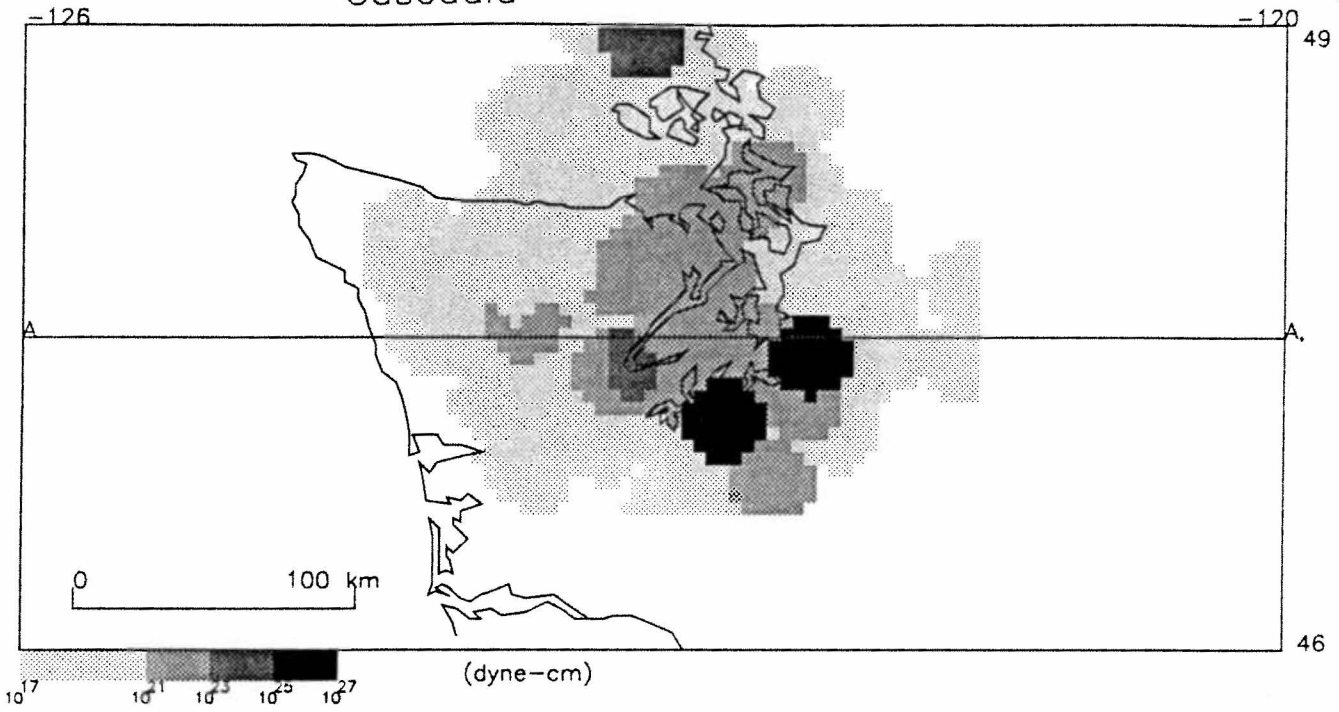

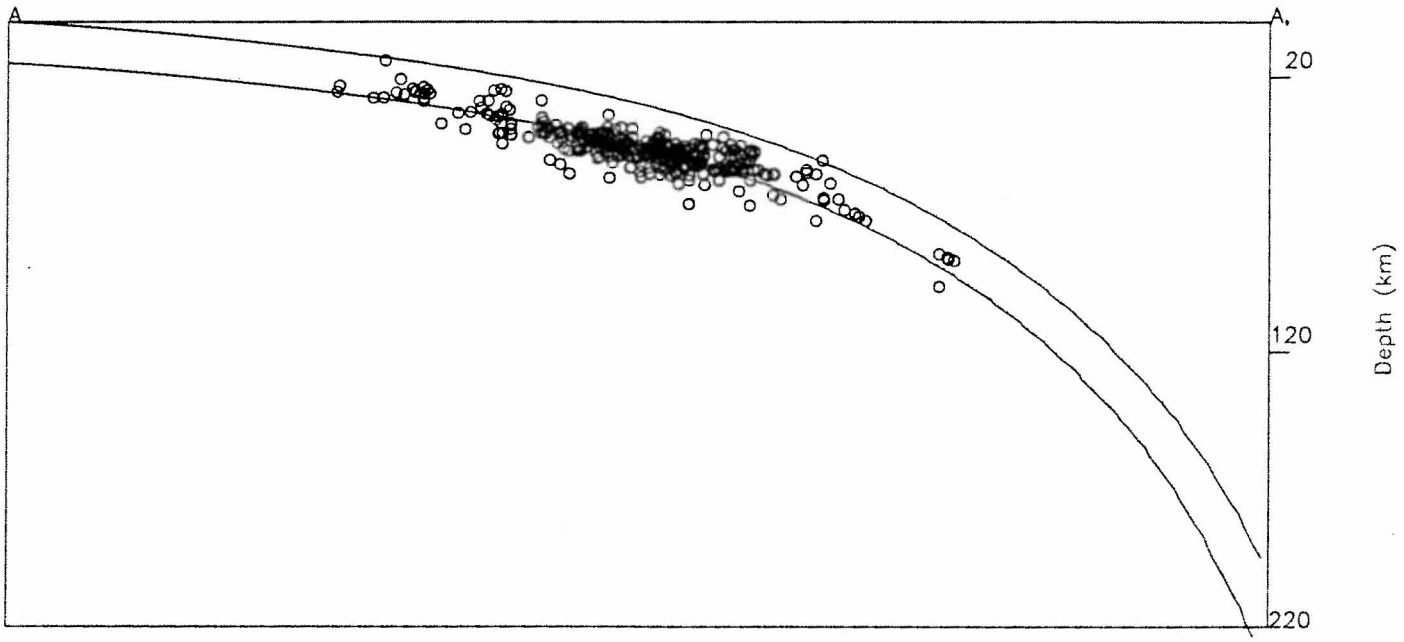

Fig 4. (top) Seismic moment density diagram for the Cascadia subduction zone. The seismic moments of all intraslab events that lie within 20 km of each point are summed and displayed using a logarithmic grey scale. The two black dots are earthquakes with m_B magnitudes of 6.9 and 7.1 and represent 99% of the seismic moment during the last 40 years. Even though the smaller events represent relatively insignificant moment, their geographic distribution shows a concentration in the vicinity of the predicted high strain-rate area of Figure 3. (bottom) Cross section AA' showing slab seismicity (circles) and the slab shape that minimizes bending strain rates of equation (4) Upper curve represents the contact between the subducting and overriding plates. Lower curve is the mid-plane of the seismogenic zone. This smooth slab goes through the trench at the right place, through the region of deep, high seismic velocity imaged by Rasmussen and Humphreys [1988], and through the seismicity if we assume the seismicity occurs beneath the subducted oceanic moho. Mean strain rates are 2×10^{-1} s^{-1}.

km and a presumed slab thickness of 10 km (the apparent seismogenic thickness determined from seismicity distributions) this seismic moment can be scaled using (8) to either an in-plane or mean bending strain rate of $4\times 10^{-16}s^{-1}$. This observation along with the theoretical calculations suggest that both bending and in-plane strain rates are important in the deformation of the Cascadia slab, that the geographic distribution of slab events can be explained by the concentration of in-plane strains forced by the backwards curvature of the trench, and that the rate of deformation estimated from seismic moments is the same order of magnitude as the bending and in-plane strain rates predicted from the kinematic flow models.

Earthquake Hazards

Although the work under this project is focused primarily on fundamental studies that contribute significantly to our ability to assess earthquake hazards, we note here some work that is of more direct earthquake hazard orientation. We are currently working with Dr. Mooto Ukawa, visiting rearch scientist from Japan, in a comparison of the seismic and other characteristics of the Cascadia Subduction zone with the Philippine Sea plate subduction in southwest Japan. Dr. Ukawa has given a paper at the Spring SSA meeting presenting some preliminary results of this comparison. There is a great deal of similarity in the patterns of seismicity within restricted parts of these two subduction zones. However major differences exist in the geometry of the two subducted plates. Beneath Japan, the Philippine Sea plate is strongly curved with possible cusp-like discontinuities in slope. The Juan de Fuca plate, based on current data, appears to be relatively smoothly deformed with trench curvature of the opposite sign. The abstract of Ukawa's paper is included in Appendix 2 of this report.

In another paper that discusses regional aspects of earthquake hazards, we have finished our manuscript for the DNAG volume on seismicity (Ludwin et al., 1989). A copy of the manuscript is included in this report as Appendix 3. It is interesting to note that, although most of the larger well documented subcrustal earthquakes associated with the CSZ have been within the subducted slab of the Puget Sound region, the larger crustal events such as the 1946 Vancouver Island, the 1872 North Cascades, the 1981 Elk Lake, and the 1962 Portland earthquakes all are located

peripheral to the Puget Basin. This suggests that recurrence statistics compiled from small crustal earthquakes in the Puget Basin may not be relevant to the region as a whole. Furthermore, most of these larger crustal earthquakes have occurred in regions that are presently quiet at the microearthquake level. Thus we might speculate that the occurrence of earthquakes at the microearthquake level is providing us with information that is fundamentally different from that provided by the intermediate to large but isolated crustal earthquakes. Even though they appear to occur in proximity, similarly the large and small intraslab earthquakes may also reflect fundamentally different processes as noted from our investigation of b-values above.

Acknowledgements

Work under this grant could not be carried out without the data collected by the Washington Regional Seismographic Network. We are very grateful for the excellent work done by the WRSN electronic technicians, data analysts, and seismologists.

Publications partially or fully supported under this contract

Articles

Boyd, T.M., and K.C. Creager, 1989 (in revision), The geometry of Aleutian subduction: Three-dimensional kinematic flow modeling, JGR.

Creager, K.C., and T.M. Boyd, 1989 (in revision), The geometry of Aleutian subduction: Three-dimensional seismic imaging, JGR.

Lees, J.M. and R.S. Crosson, 1989 (in press), Bayesian ART versus conjugate gradient methods in tomographic seismic imaging: An application at Mount St. Helens, Washington, AMS-SIAM: Conference on spatial statistics and imaging - June, 1988.

Lees, J.M. and R.S. Crosson, 1989 (in press), A tomographic inversion for the 3-D velocity structure at Mount St. Helens using earthquake data, JGR.

Lees, J.M. and R.S. Crosson, 1989 (submitted), Tomographic imaging of local earthquake delay times for 3-D velocity variation in western Washington, JGR

Ludwin, R. S., S.D. Malone, R.S. Crosson, 1988, Washington Earthquakes 1984, in U.S. Earthquakes, National Earthquake Information Service.

Ludwin, R. S., S.D. Malone, R.S. Crosson, A.I. Qamar, 1989 (in press), Washington Earthquakes 1985, in U.S. Earthquakes, National Earthquake Information Service.

Ludwin, R. S., S.D. Malone, R.S. Crosson, A.I. Qamar, 1989 (in press), Washington Earthquakes

1986, in U.S. Earthquakes, National Earthquake Information Service.

Ludwin, R. S., C.S. Weaver, and R.S. Crosson, 1989 (in press), Seismicity and Tectonics of the Pacific Northwest, in: Slemmons, D.B., E.R. Engdahl, D. Shwartz, and M. Zoback editors, Decade of North American Geology associated volume GSMV-1; Neotectonics of North America.

McCrumb, D.R., R.W. Galster, R.S. Crosson, R.S. Ludwin, D.O. West, W.E. Hancock, and L.V. Mann, 1989 (in press), Tectonics, Seismicity, and Engineering Seismology in Washington, in Association of Engineering Geologists, Washington State Centennial Volume.

VanDecar, J.C. and R. S. Crosson, 1989 (in revision), Determination of teleseismic relative phase arrival times using multi-channel cross correlation and least squares, BSSA.

Theses

Lees, J.M., 1989, Seismic Tomography in Western Washington, University of Washington, Ph.D. dissertation, 173 p.

Reports

Univ. of Wash. Geophysics Program, 1988, Quarterly Network Report 88-C on Seismicity of Washington and Northern Oregon

Univ. of Wash. Geophysics Program, 1989, Quarterly Network Report 88-D on Seismicity of Washington and Northern Oregon

Univ. of Wash. Geophysics Program, 1989, Quarterly Network Report 89-A on Seismicity of Washington and Northern Oregon

Final Technical Report: 1988, 1989 (in preparation), Earthquake Hazard Research in the Pacific Northwest, USGS Grant #14-08-0001-G1390.

Abstracts

Chiao, L.-Y., K.C. Creager, and T.M. Boyd, 1989, Membrane and bending strains associated with subduction of the Cascadia slab, Seis. Res. Let., V. 60(1), p. 2.

Creager, K.C., and T.M. Boyd, 1988, 3-D Kinematic Slab Flow in the Aleutians, EOS, V. 69(44), p. 1438.

Crosson, R.S., 1989, Testing the arch model for slab geometry of the Cascadia subduction zone in the vicinity of Puget Sound, Washington, Seis. Res. Lett., V. 60(1), p. 2.

Crosson, R.S., and J.M. Lees, 1989, Regularization or smoothing in inversion and seismic tomography as a linear filtering operation, EOS, V. 70(20), p. 602.

Lees, J.M. and Crosson, R.S., 1988, Bayesian ART versus conjugate gradient tomographic imaging in application to delay times from local earthquakes in western Washington, EOS, V. 69(44), p. 1308.

Lees, J.M. and Crosson, R.S., 1989, Tomographic imaging of local earthquake delay times for 3-

D velocity variations in western Washington, EOS, V. 70(9), p. 139.

Lees, J.M. and J.C. VanDecar, 1989, Seismic tomography constrained by Bouguer gravity anomalies, Seis. Res. Let. Vol. 60(1), p. 11.

Ludwin, R.S., C.S. Weaver, and R.D. Catchings, 1989, Apparent structural relations between crustal earthquakes and continental rifting in the Columbia Plateau, Washington, Seis. Res. Lett., V. 60(1), p. 29.

REFERENCES

Astiz, L., T. Lay, and H. Kanamori, Large intermediate-depth earthquakes and the subduction process, Phys. Earth Planet. Inter., 53, 80-166, 1988.

Baker, G. E., and C. A. Langston, Source parameters of the 1949 magnitude 7.1 south Puget Sound, Washington earthquake as determined from long-period body waves and strong ground motions, Bull. Seismol. Soc. Am., 77, 1530-1557, 1987.

Bevis, M., Seismic slip and down-dip strain rates in Wadati-Benioff zones, Science, 240, 1317-1319, 1988.

Brune, J. N., Seismic moment, seismicity, and rate of slip along major fault zones., J. Geophys. Res., 73, 777-784, 1968.

Caldwell, J. G., W. F. Haxby, D. E. Karig, and D. L. Turcotte, On the applicability of a universal elastic trench profile, Earth Planet. Sci. Lett., 31, 239-246, 1976.

Chapple, W. M., and D. W. Forsyth, Earthquakes and bending of plates at trenches, J. Geophys., Res., 84, 6729-6749, 1979.

Crosson, R. S., and T. J. Owens, Slab geometry of the Cascadia subduction zone beneath Washington from earthquake hypocenters and teleseismic converted waves. Geophys. Res. Lett., 14, 8, 824-827, 1987.

Crosson, R.S. and J.M. Lees, Regularization or smoothing in inversion and seismic tomography as a linear filtering opera- tion (abstract), EOS, 70, 601, 1989.

Goetze, C., The mechanism of creep in Olivine, Phil. Trans. R. Soc. Lond., A288, 99-199, 1978.

Hori, S., H. Inoue, Y. Fukao, M. Ukawa, Seismic detection of the untransformed 'basaltic' oceanic crust subducting into the mantle, Geophys. J. R. Astr. Soc. 83, 169-197, 1985.

Houseman, G. and P. England, Finite strain calculations of continental deformation 1. Method

and general results for convergent zones, J. Geophys. Res., 91, 3651- 3663, 1986.

Kawakatsu, H., Double seismic zones: Kinematics, J. Geophys. Res., 91, 4811- 4825, 1986.

Lees, J.M. and Crosson, R.S., Tomographic imaging of local earthquake delay times for 3-D velocity variations in western Washington (abstract), EOS , 70(9), 139, 1989.

Lees, J.M. and J.C. VanDecar, Seismic tomography constrained by Bouguer gravity anomalies (abstract), Seis. Res. Letts., 60, 11, 1989.

Ludwin, R.S., C.S. Weaver, and R.S. Crosson, Seismicity of the Pacific Northwest, Decade of North American Geology associated volume GSMV-1; Neotectonics of North America, (in revision) 1989.

McAdoo, D. C., J. G. Caldwell, and D. L. Turcotte, On the elastic-perfectly plastic bending of the lithosphere under generalized loading with application to the Kuril trench, Geophys. J. R. Astr. Soc., 54, 11-26, 1978.

Meyerholtz, K.A., G.L. Pavlis, and S.A. Szpakowski, Convolutional quelling in seismic tomography, Geophysics, 54, 570-580, 1989.

Paige and Saunders, LSQR an algorithm for sparse linear equations, ACM trans. math software, 8, 43-71, 1982.

Rasmussen, J. and E. Humphreys, Tomographic image of the Juan De Fuca plate beneath Washington and Western Oregon using teleseismic P-wave travel times, Geophys. Res. Lett., 15, 1417-1420, 1988.

Rodi, W.L., T.H. Jordan, J.F. Masso, J.M. Savino, Determination of three-dimensional structure of Eastern Washington from the joint inversion of gravity and earthquake travel time data, Systems, Science and Software, Technical Report, Project No. 40094, 1980.

Tsukahara, H., Physical conditions for double seismic planes of the deep seismic zone, J. Phys. Earth, 28, 1-15, 1980.

Vassiliou, M. S., B. H. Hager, and A. Raefsky, The distribution of earthquakes with depth and stress in subducting slabs, J. Geodynamics, 1, 11-28, 1984.

Weaver, C.S. and G.E. Baker, Geometry of the Juan de Fuca plate beneath Washington and northern Oregon from seismicity, Bull. Seis. Soc. Am., 78, 264-275, 1988.